A MATHEMATICAL MODEL OF RAT VENTRICULAR CARDIOMYOCYTE WITH A NOVEL DESCRIPTION OF INTRACELLULAR AND T-TUBULAR Ca^{2+} DYNAMICS

Michal Pásek*,**, Jiří Šimurda**

In this paper, we present a novel quantitative description of intracellular and t-tubular Ca^{2+} dynamics in a model of rat cardiac ventricular myocyte. In order to simulate recently published data, the model incorporates t-tubular and peripheral dyads and intracellular subspaces, segmentation of the t-tubular luminal volume, reformulation of the inactivation properties of t-tubular and peripheral L-type calcium current (I_{Ca}) and a description of exogenous Ca^{2+} buffer function in the intracellular space. The model is used to explore activity-induced changes of ion concentrations in the intracellular and t-tubular spaces and their role in excitation – contraction coupling in ventricular myocytes.

Keywords: *cardiac cell, intracellular Ca^{2+} dynamics, t-tubule, quantitative modelling*

1. Introduction

The mechanical activity (contractions) of cardiac myocytes is triggered indirectly by electrical activity (action potentials). The signal mediating the coupling between electrical excitation and contraction is carried by calcium ions (Ca^{2+}) stored in the terminal part of sarcoplasmic reticulum (SR) and released during each period to cytosolic space. Binding transiently to contractile proteins they control development of muscle contraction [1]. The magnitude and time course of transient changes in cytosolic Ca^{2+} concentration (shortly $[Ca^{2+}]_c$-transient) is therefore regarded as a principal measurable signal in the process of excitation-contraction coupling. Exploration of the factors potentially affecting $[Ca^{2+}]_c$-transient and consequently contraction is thus important. A significant role may be played by activity-induced changes of ion concentrations in the lumen of the t-tubular system that are not measurable by contemporary methods but can be explored by use of quantitative models. In 2006 we published the first mathematical model of rat cardiac ventricular myocyte including a quantitative description of the transverse (t-) tubular system [2]. The model was used to explore activity-induced changes of ion concentrations in the t-tubular lumen and their role in modulating the electrical and mechanical activity of the myocyte. However, recent experimental data have shown that Ca^{2+} transport through cellular membrane and Ca^{2+} dynamics in the intracellular and t-tubular spaces are more complex [3, 4, 5, 6, 7] than described in the model. In the current work, we present a modified model of rat ventricular myocyte that includes a novel description of intracellular and t-tubular Ca^{2+} dynamics enabling the recent findings to be incorporated. The principal modifications to

* doc. Ing. M. Pásek, Ph.D., Institute of Thermomechanics – Branch Brno, Czech Academy of Science, Brno, Czech Republic

** doc. Ing. M. Pásek, Ph.D., doc. RNDr. Ing. J. Šimurda, CSc., Department of Physiology, Masaryk University, Brno, Czech Republic

the original model [2] include: (i) partition of the original single dyadic space into two: one adjacent to surface membrane and second adjacent to t-tubular membrane; (ii) incorporation of peripheral and t-tubular intracellular subspaces; (iii) partition of the t-tubule luminal volume into nine concentric segments; (iv) reformulation of calcium current (I_{Ca}) inactivation to reproduce its different characteristics at the surface and t-tubular membranes; (v) incorporation of a quantitative description of the function of exogenous Ca^{2+} buffers in the intracellular space.

2. Modification of the Model

2.1. Model structure

The modified model is illustrated in Fig. 1. The presence of peripheral dyads [3] and ion gradients under the membrane [8] is taken into account by incorporation of the following new compartments: dyadic space adjacent to surface membrane (surface dyadic space); junctional sarcoplasmic reticulum adjacent to surface dyadic space (JSR_s) and subsarcolemmal spaces adjacent to surface and t-tubular membranes (surface subsarcolemmal space and tubular subsarcolemmal space).

The total volume of the model cell (V_{tot}) was set to 11.14 pL. The volumes of the intracellular compartments are specified in Tab. 1. Because of the lack of experimental data, we assumed that the fractional volumes of dyadic space and SR release compartment adjacent to the t-tubular membrane ($f_{Vd,t}$, $f_{VJSR,t}$) are comparable to the t-tubular fraction of I_{Ca} ($f_{Vd,t} = f_{VJSR,t} = f_{Ca,t} = 0.8$ [3]). The fractional volumes of surface and t-tubular submembrane spaces ($f_{Vs,s} = 0.65$ and $f_{Vs,t} = 0.35$, respectively) were set to be proportional to the non-junctional area of each membrane (92.3 % of surface membrane and 52 % of t-tubular membrane [4]).

Symbol	Specification	Value [pl]
V_c	cytosolic space	6.2937
$V_{s,s}$	surface subsarcolemmal subspace	0.1440
$V_{s,t}$	tubular subsarcolemmal subspace	0.0775
$V_{d,s}$	surface dyadic space	0.0001420
$V_{d,t}$	tubular dyadic space	0.0005679
$V_{JSR,s}$	surface junctional compartment of sarcoplasmic reticulum	0.0078
$V_{JSR,t}$	tubular junctional compartment of sarcoplasmic reticulum	0.0312
V_{NSR}	network compartment of sarcoplasmic reticulum	0.3508

Tab.1: Volumes of intracellular compartments

The total volume of the t-tubular system in the model cell represents the sum of the volumes of all t-tubules; the percentage volume of the t-tubular system is 3.3 % [9] and the percentage area of t-tubular membrane is 49 % [5]. To simulate ion gradients in the t-tubular lumen, and thus ion concentrations adjacent to the t-tubule membrane, the system ('each t-tubule') was partitioned into 9 concentric cylindrical segments S_{t1}, S_{t2}, ... , S_{t9} (Fig. 1, bottom). To increase the accuracy of computation of ion concentrations close to the t-tubular membrane, the volumes of segments $S_{t1} - S_{t8}$ were set to 3 % of the total tubular volume.

The specific capacitances of the t-tubular and surface membranes were set to $0.714\,\mu F/cm^2$ and $1.275\,\mu F/cm^2$, respectively. This is consistent with the results of experimental and simulation studies published in [5].

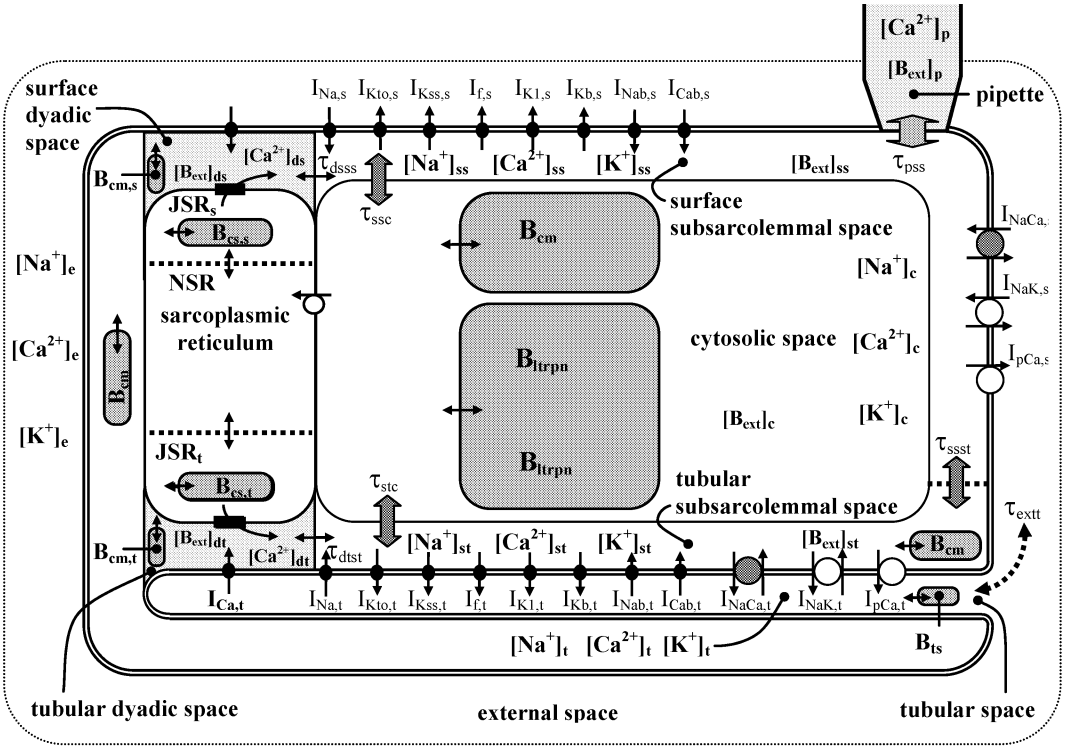

Fig.1: Schematic diagram of the rat ventricular cell model used in the present study. The description of the electrical activity of surface (s) and t-tubular (t) membranes comprises formulations of the following ionic currents: fast sodium current (I_{Na}), L-type calcium current (I_{Ca}), transient outward potassium current (I_{Kto}), steady-state outward potassium current (I_{Kss}), inward rectifying potassium current (I_{K1}), hyperpolarization-activated current (I_{f}), background currents (I_{Kb}, I_{Nab}, I_{Cab}), sodium-calcium exchange current (I_{NaCa}), sodium-potassium pump current (I_{NaK}) and calcium pump current (I_{pCa}). The intracellular space contains the cytosolic space (c), surface and tubular subsarcolemmal subspaces (ss, st), surface and tubular dyadic spaces (dt, ds), network and junctional compartments of sarcoplasmic reticulum (NSR, JSR_{s}, JSR_{t}), endogenous Ca^{2+} buffers (calmodulin (B_{cm}), troponin (B_{htrpn}, B_{ltrpn}), calsequestrin (B_{cs})) and exogenous Ca^{2+} buffer (e.g. BAPTA or EGTA; B_{ext})). The tubular space is partitioned into nine concentric segments, $S_{\mathrm{t1}} - S_{\mathrm{t9}}$; a schematic representation of this partitioning is shown under the diagram. B_{ts} denotes the non-specific Ca^{2+} buffer associated with luminal part of tubular membrane. J_{up} represents Ca^{2+} flow via SR Ca^{2+} pump and the small filled rectangles in JSR membrane ryanodine receptors. The small bi-directional arrows denote Ca^{2+} diffusion. Ion diffusion between the tubular and external space is represented by the dashed arrow.

2.2. Membrane transport system

Voltage dependent inactivation (VDI) and Ca^{2+} dependent inactivation (CDI) of I_{Ca} were reformulated on the basis of the experimental results in [3] which showed faster inactivation of I_{Ca} in the t-tubules than in the peripheral membrane, as a result of more efficient CDI in response to Ca^{2+} released at the t-tubules. All parameters of CDI are regarded as dependent on the level of calmodulin saturation with Ca^{2+} ($B_{cm,Casat}$, [8]). The steady state levels and time constants of VDI (ss_{VDI}, τ_{VDI}) and CDI (ss_{CDI}, $\tau_{CDI,s}$, $\tau_{CDI,t}$) are described by the following equations:

$$ss_{VDI,x} = \frac{1}{1+e^{((V_{m,x}+26.7)/5.4)}},$$

$$\tau_{VDI,x} = \frac{0.04715}{e^{((V_{m,x}+47)/12)^2}} + \frac{0.092}{1+e^{(-(V_{m,x}+55)/5)}} + \frac{0.01725}{1+e^{((V_{m,x}+75)/25)}},$$

$$ss_{CDI,x} = \frac{1}{1+0.244\left(\frac{B^4_{cm,Casat,x}+0.318^4}{B^4_{cm,Casat,x}}\right)},$$

$$\tau_{CDI,s} = 0.014 + \frac{0.029}{1+e^{((B_{cm,Casat,s}-0.77)/0.075)}},$$

$$\tau_{CDI,t} = 0.0005 + \frac{0.0285}{1+e^{((B_{cm,Casat,t}-0.77)/0.07)}}.$$

While the formulations of ss_{VDI}, τ_{VDI} and ss_{CDI} in the description of $I_{Ca,s}$ and $I_{Ca,t}$ are identical (the suffix x in the equations stands for s (surface) or t (tubular)), the τ_{CDI} of these two currents is formulated differently (see $\tau_{CDI,s}$ and $\tau_{CDI,t}$); this takes into account the observed different modulation of surface and t-tubular I_{Ca} by Ca^{2+} released from SR [3].

The fractions of ion transporters in the t-tubular membrane (Tab. 2) were set according to [5] except for the values of $f_{Ca,t}$ and $f_{pCa,t}$ which were set to 0.8 [3] and 0.95 [6], respectively.

The permeability of I_{Ca}-channels and conductivity of I_{to}-channels were increased by 10 % and 20 %, respectively, to provide better agreement of simulated I_{Ca} with experimental data (12.6 pA/pF, [3]) and action potentials of physiological duration.

$f_{Na,t}$	0.38	$g_{Na,max}$	$10\,mS\,cm^{-2}$
$f_{Ca,t}$	0.80	P_{Ca}	$0.00023\,cm\,s^{-1}$
$f_{Kto,t}$	0.46	$g_{Kto,max}$	$0.420\,mS\,cm^{-2}$
$f_{Kss,t}$	0.86	$g_{Kss,max}$	$0.070\,mS\,cm^{-2}$
$f_{K1,t}$	0.47	$g_{K1,max}$	$0.240\,mS\,cm^{-2}$
$f_{f,t}$	0.49	$g_{f,max}$	$0.015\,mS\,cm^{-2}$
$f_{Nab,t}$	0.49	$g_{Nab,max}$	$0.802\,\mu S\,cm^{-2}$
$f_{Cab,t}$	0.49	$g_{Cab,max}$	$0.648\,\mu S\,cm^{-2}$
$f_{Kb,t}$	0.49	$g_{Kb,max}$	$1.380\,\mu S\,cm^{-2}$
$f_{NaCa,t}$	0.78	k_{NaCa}	$0.18\,nA\,cm^{-2}\,mM^{-4}$
$f_{NaK,t}$	0.64	$I_{NaK,max}$	$1.00\,\mu A\,cm^{-2}$
$f_{pCa,t}$	0.95	$I_{pCa,max}$	$0.85\,\mu A\,cm^{-2}$

$f_{X,t}$ represents the t-tubule fraction of the ion transporter underlying current I_X. $g_{X,max}$, $I_{X,max}$ or P_X denote maximum conductivity, current or permeability of each ion transport system, respectively, related to total membrane area.

Tab.2: Electrical properties of ion transport systems

2.3. Intracellular Ca^{2+}-handling

The function of ryanodine receptors (RyR) in JSR was formulated as described in [8], although the values of k_s and k_{oCa} were increased to $250\,ms^{-1}$ and $50\,mM^{-2}\,ms^{-1}$ respectively, so that dyadic Ca^{2+} transients reached $\sim 100\,\mu M$ when $[Ca^{2+}]_{NSR} = 0.5\,mM$ [8], [10]. The description of the SR Ca^{2+} pump (originally adopted from [11]) was modified to be consistent with the data in [12]; the constants used are: $K_{SR} = 1$, $v_{maxf} = v_{maxr} = 0.296\,\mu mol/l$ cytosol/s, $K_{fb} = 168\,nM$, $K_{rb} = 1.176\,mM$, $N_{fb} = 1.2$ and $N_{rb} = 1.287$. The Ca^{2+} dissociation constant of calsequestrin ($K_{d,Bcs}$) in JSR was decreased to 0.65 mM [8] and Ca^{2+} buffering by calmodulin was described using $k_{on,Bcm} = 100000\,mM^{-1}\,s^{-1}$ and $k_{off,Bcm} = 238\,s^{-1}$ [13].

The model was supplemented by a description of exogenous Ca^{2+} buffer (EGTA) diffusion among the pipette, subsarcolemmal spaces, dyadic spaces and cytosol (rate constants: $k_{on,Bext} = 5000\,mM^{-1}\,s^{-1}$, $k_{off,Bext} = 0.75\,s^{-1}$). The time constants controlling the rate of diffusion of exogenous Ca^{2+} buffer and of Ca^{2+} between individual cellular compartments are specified in Tab. 3.

Symbol	Value [s]		Symbol	Value [s]	
$\tau_{pss,buffer\text{-}free}$	4.42	(i)	$\tau_{ssc,buffer\text{-}free}$	0.00175	(iii)
$\tau_{pss,buffer\text{-}Ca}$	4.42	(i)	$\tau_{ssc,buffer\text{-}Ca}$	0.00175	(iii)
$\tau_{pss,Ca}$	4.42	(i)	$\tau_{ssc,Ca}$	0.00175	(iii)
$\tau_{dsss,buffer\text{-}free}$	0.34E−3	(ii)	$\tau_{stc,buffer\text{-}free}$	0.00325	(iv)
$\tau_{dsss,buffer\text{-}Ca}$	0.34E−3	(ii)	$\tau_{stc,buffer\text{-}Ca}$	0.00325	(iv)
$\tau_{dsss,Ca}$	1.1E−3	(ii)	$\tau_{stc,Ca}$	0.00325	(iv)
$\tau_{dtst,buffer\text{-}free}$	0.34E−3	(ii)	$\tau_{ssst,buffer\text{-}free}$	0.1	(v)
$\tau_{dtst,buffer\text{-}Ca}$	0.34E−3	(ii)	$\tau_{ssst,buffer\text{-}Ca}$	0.1	(v)
$\tau_{dtst,Ca}$	0.15E−3	(ii)	$\tau_{ssst,Ca}$	0.1	(v)

(i) Time constants of diffusion from the pipette to surface subspace were set to reproduce approximately the increase of $[Ca^{2+}]_c$ observed in isolated cells loaded with $100\,\mu M$ fura 2 after membrane rupture using a pipette ($3\,M\Omega$) filled with 3 mM EGTA and 170 nM free Ca^{2+} (unpublished data courtesy of Professor G. L. Smith, University of Glasgow). (ii) Time constants of diffusion from the dyadic spaces to corresponding subspaces were set for $[Ca^{2+}]_c$ to reach a peak within 20 ms from the start of stimulation at all stimulation rates. (iii, iv) Time constants of diffusion from the surface and tubular subspaces to cytosolic space were set to generate a Ca^{2+} gradient under the membrane [3]. The ratio $\tau_{stc,Ca}/\tau_{ssc,Ca}$ reflects the ratio of non-junctional areas of the surface and tubular membrane (65 % / 35 % – derived using data in [4]). (v) Time constants of diffusion from the surface subspace to tubular subspace were set at the minimum value that prevents a physiologically significant interaction between the compartments. Time constants represent the time needed for the ion concentration in the second compartment to undertake 63 % of the difference between its final and initial values after a rapid change of ion concentration in the first compartment. The time constants for intracellular Na^+ and K^+ diffusion were set to the same values as for Ca^{2+} diffusion.

Tab.3: Time constants related to intracellular transport of Ca^{2+} and Ca^{2+}-buffers

2.4. Ion exchange within t-tubules and between t-tubules and the external space

The time constants for Ca^{2+} and K^+ exchange between the t-tubule segments and the external solution ($\tau_{Ca,extt}$, $\tau_{K,extt}$) were adjusted to reproduce the changes of I_{Ca} and resting potential observed experimentally following a rapid change of external bulk ion concentrations at 36 °C [7]. The time constants controlling Ca^{2+} and K^+ exchange between the individual t-tubular segments were computed by multiplying the $\tau_{Ca,extt}$ and $\tau_{K,extt}$ by

a factor that takes into account the different diffusion area between individual segments and, in segments S_{t8} and S_{t9}, their different volumes. The resulting formulation is:

$$\tau_{X,St,n+1} = \tau_{X,extt} \frac{A_{base,n}}{A_{boundary,n}} \frac{V_{St,n+1}}{V_{St,n}} ,$$

where $\tau_{X,St,n+1}$ represent the time constant controlling the rate of diffusion of ion X from segment n to segment $n+1$ and the parameters $A_{base,n}$, $A_{boundary,n}$, $V_{St,n+1}$ and $V_{St,n}$ represent the area of segment n in the tubular mouth, area of the boundary between segments n and $n+1$, volume of segment $n+1$ and volume of segment n, respectively.

The time constant $\tau_{Na,extt}$ is considered to be equal to $\tau_{K,extt}$ and, because the concentration changes of tubular Na^+ are minimal, they are described in a single t-tubule compartment, as in our original work [2].

To reconstruct the biphasic decrease of I_{Ca} observed following a rapid decrease of $[Ca^{2+}]$ in the external bulk solution (Fig. 2), the model was modified to include a Ca^{2+} buffer (B_{ts}) in t-tubular segment S_{t1}. Optimising the model using the same pulse and solution change protocol used experimentally gave the following values for buffer parameters and time constants of Ca^{2+} exchange: $k_{on,Bts} = 2\,s^{-1}\,Mm^{-1}$, $k_{off,Bts} = 2.6\,s^{-1}$, $[B_{ts}] = 93.6\,mM$ and $\tau_{Ca,extt} = 170\,ms$. To fit the change of resting membrane potential observed experimentally after a rapid change of external $[K^+]$ from 4.4 to 6.6 mM (see Fig. 1 in [7]) the time constant $\tau_{K,extt}$ had to be set to 150 ms.

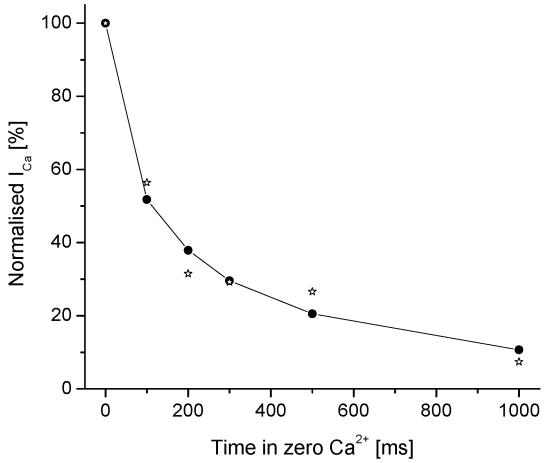

Fig.2: Model reconstruction of the experimental data of Yao et al. [7] showing a decline in I_{Ca} following rapid exposure of a myocyte to Ca^{2+}-free external solution at 37 °C. The initial external concentration of Ca^{2+} was 1.08 mM. The experimental data are represented by asterisks and the results from the model by filled circles.

Finally, the time constants were corrected for the lower temperature of the model cell (22 °C, $Q_{10} = 1.3$, [14]) to give the values: $\tau_{Ca,extt} = 252\,ms$ and $\tau_{Na,extt} = \tau_{K,extt} = 222\,ms$.

2.5. Numerical integration technique

The model was implemented in the program MATLAB 6.5 and numerical computation of the system of 97 differential equations was performed using the solver for stiff systems

ODE-15s. The model was run for 10 minutes of equivalent cell lifetime to ensure that steady-state was reached. The values of all variables at this time were assigned as starting values before running model trials. The basic units in which the equations were solved were: mV for membrane voltage, μA for membrane currents, mM for ionic concentrations, s for time, and ml for volumes.

3. Results

The Ca^{2+} dynamics of the model cell at steady state 5 Hz stimulation (corresponds to the resting heart rate of rat) is illustrated in Fig. 3. The left panel shows t-tubule (dotted lines) and surface membrane (solid lines) action potentials and Ca^{2+}-carrying currents (I_{Ca}, I_{NaCa}, I_{pCa}, I_{Cab}). The action potentials are almost identical as a consequence of tight electrical coupling between the two membrane systems. However, there are marked differences between the t-tubular and surface components of Ca^{2+} currents resulting from predominant localisation of Ca^{2+} transporting proteins in the t-tubular membrane (see Tab. 2) and partly from changes of Ca^{2+} concentrations in the t-tubule lumen ($[Ca^{2+}]_{t1}$). The upper graph of right panel shows Ca^{2+} concentrations in the 1st, 3rd, 5th, 7th and 9th segments of the t-tubule lumen, showing that the changes of $[Ca^{2+}]$ are greatest in the vicinity of t-tubular membrane and decrease towards the centre of the t-tubule. Thus, during activity, a radial ion concentration gradient arises in the t-tubule lumen as a result of trans-membrane Ca^{2+} fluxes, which, in turn, are altered by ion concentration changes in t-tubules. The remaining graphs of the right panel illustrate the Ca^{2+} concentration changes in the network and re-

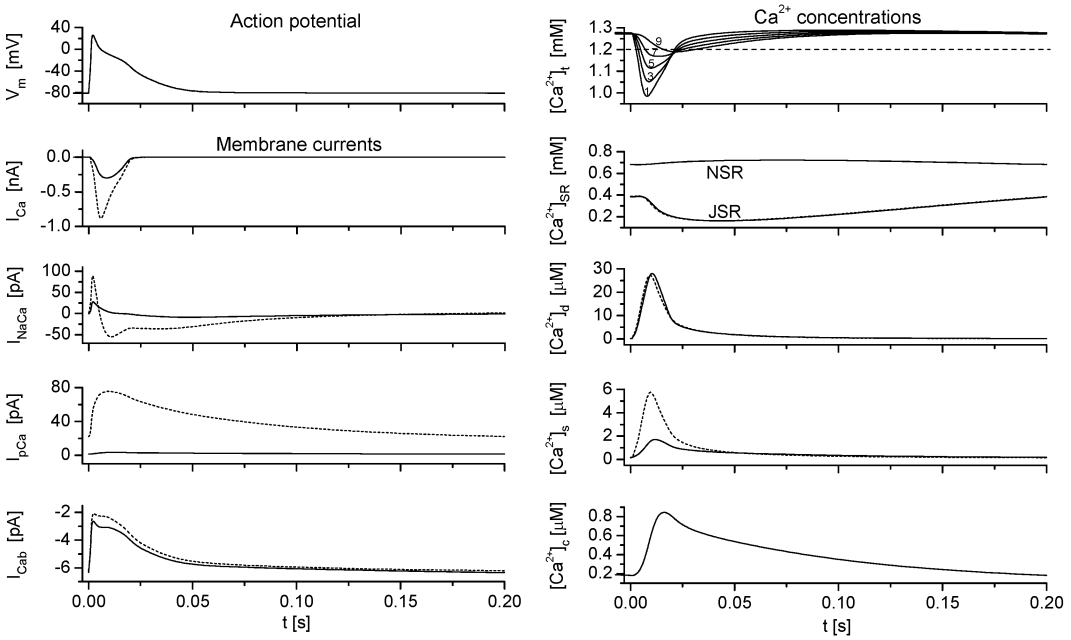

Fig.3: Action potentials (V_m), Ca^{2+} currents (I_{Ca}, I_{NaCa}, I_{pCa}, I_{Cab}) and Ca^{2+} concentrations in t-tubular ($[Ca^{2+}]_{t1}$, $[Ca^{2+}]_{t3}$, $[Ca^{2+}]_{t5}$, $[Ca^{2+}]_{t7}$, $[Ca^{2+}]_{t9}$) and intracellular spaces ($[Ca^{2+}]_{NSR}$, $[Ca^{2+}]_{JSR}$, $[Ca^{2+}]_{ds}$, $[Ca^{2+}]_{dt}$, $[Ca^{2+}]_{ss}$, $[Ca^{2+}]_{st}$, $[Ca^{2+}]_{c}$) at 5 Hz steady state stimulation. Solid lines refer to peripheral membrane and dotted lines to t-tubular membrane. The horizontal dashed line in the panel of $[Ca^{2+}]_t$ indicates external Ca^{2+} concentration (1.2 mM).

lease compartments of SR and the presence of a $[Ca^{2+}]$ gradient at the intracellular side of cell membrane; the activity induced changes of intracellular Ca^{2+} concentrations are greatest under the membrane (compare the magnitudes of changes in $[Ca^{2+}]_d$ and $[Ca^{2+}]_s$ with substantially smaller Ca^{2+} transient at the level of sarcomere (see $[Ca^{2+}]_c$)).

To investigate the effect of radial Ca^{2+} concentration gradient in the t-tubule lumen on systolic Ca^{2+} transient in the cytosol, the simulation was repeated under conditions of ion concentrations in t-tubules fixed at external levels, and when t-tubular $[Ca^{2+}]$ was formulated in a single compartment. The results (Fig. 4) showed that the Ca^{2+} depletion near the t-tubular membrane (the first segment of t-tubular lumen) reduces the transmembrane Ca^{2+} flux into the cell and Ca^{2+} load in the sarcoplasmic reticulum, thus reducing the magnitude of systolic Ca^{2+} transient (peak $[Ca^{2+}]_c$ decreased by 11.3 %) compared with that observed when t-tubular $[Ca^{2+}]$ was fixed at external level or described in a single compartment.

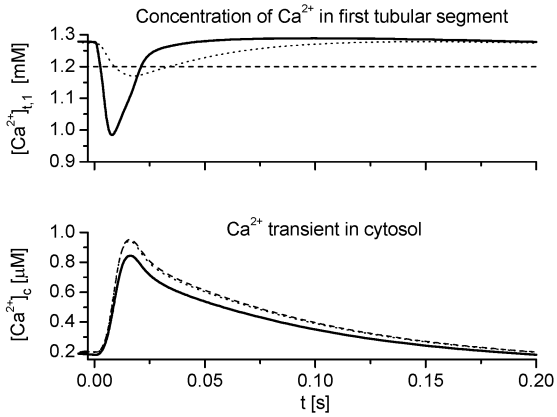

Fig.4: Cumulative effect of Ca^{2+} depletions in the first t-tubule segment on the magnitude of steady state systolic Ca^{2+}-transient in the cytosol during an action potential at a stimulation frequency of 5 Hz. The solid and dashed lines represent the results from the model with tubular ion concentrations allowed to change and fixed at external bulk levels, respectively. The dotted line shows the results when $[Ca^{2+}]_t$ was formulated in a single (non segmented) compartment.

4. Discussion and Conclusions

Quantitative models of cardiac cells are constantly being refined on the basis of new experimental findings. Conversely, such models make it possible to reconstruct processes that are currently inaccessible to experimental investigation. The aim of this work was to modify our existing model of rat ventricular myocyte [2] by incorporating recently published experimental results. The new model allows detailed investigation of the effects of activity-induced changes of ion concentrations in the intracellular and t-tubular spaces on the processes underlying electro-mechanical coupling in these cells, as illustrated in Figs. 3 and 4.

This study highlights a potentially important role of radial ion concentration gradients in t-tubular lumen in modulation of the transmembrane ion flux, intracellular Ca^{2+} load and cellular contractility. It also suggests that under physiological conditions the distribution

of ionic currents between the surface and t-tubular membranes and the changes of ion concentrations in the t-tubular system help to maintain Ca^{2+} homeostasis in cardiac cells. In future work, we intend to use this improved model to investigate the possible consequences of pathological changes in t-tubule structure and function reported in cardiac cells.

Acknowledgment

This study was realised with the institutional support RVO:61388998 and with the support of the project MUNI/A/0951/2012.

Appendix

Abbreviations used in the text

Symbol	Definition
SR	Sarcoplasmic reticulum
NSR	Network compartment of SR
JSR	Junctional compartment of SR
RyR	Ryanodine receptor

Variables used in the text

Symbol	Definition
V_{m}	Membrane voltage
I_{Na}	Fast Na^+ current
I_{Ca}	L-type Ca^{2+} current
I_{K1}	Inward rectifying K^+ current
I_{Kto}	Transient outward K^+ current
I_{Kss}	Steady-state outward K^+ current
I_{f}	Hyperpolarization-activated current
I_{Kb}	Background K^+ current
I_{Nab}	Background Na^+ current
I_{Cab}	Background Ca^{2+} current
I_{NaCa}	Na^+ – Ca^{2+} exchange current
I_{NaK}	Na^+ – K^+ pump current
I_{pCa}	Ca^{2+} pump current
$I_{\mathrm{i,s}}$	Surface membrane component of current i
$I_{\mathrm{i,t}}$	Tubular membrane component of current i
J_{up}	Ca^{2+} flow via SR Ca^{2+} pump
$[\mathrm{x}]_{\mathrm{p}}$	Free concentration of substance x in the pipette
$[\mathrm{x}]_{\mathrm{e}}$	Free concentration of substance x in external space
$[\mathrm{x}]_{\mathrm{ti}}$	Free concentration of substance x in t-tubular segment i
$[\mathrm{x}]_{\mathrm{c}}$	Free concentration of substance x in cytosolic space
$[\mathrm{x}]_{\mathrm{st}}$	Free concentration of substance x in t-tubular subsarcolemmal space
$[\mathrm{x}]_{\mathrm{ss}}$	Free concentration of substance x in surface subsarcolemmal space
$[\mathrm{x}]_{\mathrm{dt}}$	Free concentration of substance x in t-tubular dyadic space
$[\mathrm{x}]_{\mathrm{ds}}$	Free concentration of substance x in surface dyadic space
$[Ca^{2+}]_{\mathrm{NSR}}$	Free concentration of Ca^{2+} in NSR
$[Ca^{2+}]_{\mathrm{JSR}}$	Free concentration of Ca^{2+} in JSR

Parameters/constants used in the text

Symbol	Definition
$\tau_{x,extt}$	Time constant of ion x diffusion from external space to t-tubule lumen
k_s	SR Ca^{2+} release rate constant
k_{oCa}	Non SR dependent transition rate constant for RyR
K_{SR}	Scaling factor for SR Ca^{2+} pump
v_{maxf}	SR Ca^{2+} pump forward rate parameter
v_{maxr}	SR Ca^{2+} pump reverse rate parameter
K_{fb}	Forward half-saturation constant for SR Ca^{2+} pump
K_{rb}	Backward half-saturation constant for SR Ca^{2+} pump
N_{fb}	Forward cooperativity constant for SR Ca^{2+} pump
N_{rb}	Reverse cooperativity constant for SR Ca^{2+} pump
k_{on}	On rate constant for ion binding
k_{off}	Off rate constant for ion binding
Q_{10}	Temperature adjustment factor

References

[1] Bers D.M.: Cardiac excitation-contraction coupling, Nature 415 (2002) 198–205

[2] Pásek M., Christé G., Šimurda J.: The functional role of cardiac t-tubules in a model of rat ventricular myocytes, Phil. Trans. R. Soc. A. 364 (2006) 1187–1206

[3] Brette F., Sallé L., Orchard C.H.: Differential modulation of L-type Ca current by SR Ca release at the t-tubules and surface membrane of rat ventricular myocytes, Circ. Res. 95 (2004) e1–e7

[4] Brette F., Sallé L., Orchard C.H.: Quantification of calcium entry at the t-tubules and surface membrane in rat ventricular myocytes, Biophys. J. 90 (2006) 381–389

[5] Pásek M., Brette F., Nelson A., Pearce C., Qaiser A., Christé G., Orchard C.H.: Quantification of t-tubule area and protein distribution in rat cardiac ventricular myocytes, Prog. Biophys. Mol. Biol. 96 (2008) 244–257

[6] Chase A., Orchard C.H.: Ca efflux via the sarcolemmal Ca ATPase occurs only in the t-tubules of rat ventricular myocytes, J. Mol. Cell. Cardiol. 50 (2011) 187–193

[7] Yao A., Spitzer K.W., Ito N., Zaniboni M., Lorell B.H., Barry W.H.: The restriction of diffusion of cations at the external surface of cardiac myocytes varies between species, Cell Calcium 22 (1997) 431–438

[8] Shannon T.R., Wang F., Puglisi J., Weber C., Bers D.M.: A mathematical treatment of integrated Ca dynamics within the ventricular myocyte, Biophys. J. 87 (2004) 3351–3371

[9] Soeller C., Cannell M.B.: Examination of the transverse tubular system in living cardiac rat myocytes by 2-photon microscopy, Circ. Res. 84 (1999) 266–275

[10] Soeller C., Cannell M.B.: Numerical simulation of local Ca movements during L-Type Ca channel gating in the cardiac diad, Biophys. J. 73 (1997) 97–111

[11] Pandit S.V., Clark R.B., Giles W.R., Demir S.S.: A model of action potential heterogeneity in adult rat left ventricular myocytes, Biophys. J. 81 (2001) 3029–3051

[12] Shannon T.R., Bers D.M.: Assessment of Intra-SR Free [Ca] and Buffering in Rat Heart, Biophys. J. 73 (1997) 1524–1531

[13] Robertson S.P., Johnson J.D., Potter J.D.: The time-course of Ca^{2+} exchange with calmodulin, troponin, parvalbumin, and myosin in response to transient changes in Ca^{2+}, Biophys. J. 34 (1981) 559–569

[14] Hille B.: Ion channels of excitable Membranes, 3rd edition, Sunderland, MA: Sinauer Associates, 2001

Received in editor's office: March 22, 2013
Approved for publishing: June 13, 2013